Supporting Information for

Self-Assembly of Giant Bottlebrush Block Copolymer Surfactants from Luminescent Organic Electronic Materials

Yonghui Wang, Feng Shao, Ethan R. Sauvé, Christopher M. Tonge, and Zachary M. Hudson

Department of Chemistry, The University of British Columbia, 2036 Main Mall, Vancouver, British Columbia, Canada, V6T 1Z1.

Tel: +1-604-822-3266; Fax: +1-604-822-2847; e-mail: zhudson@chem.ubc.ca.

Table of contents

Additional Figures

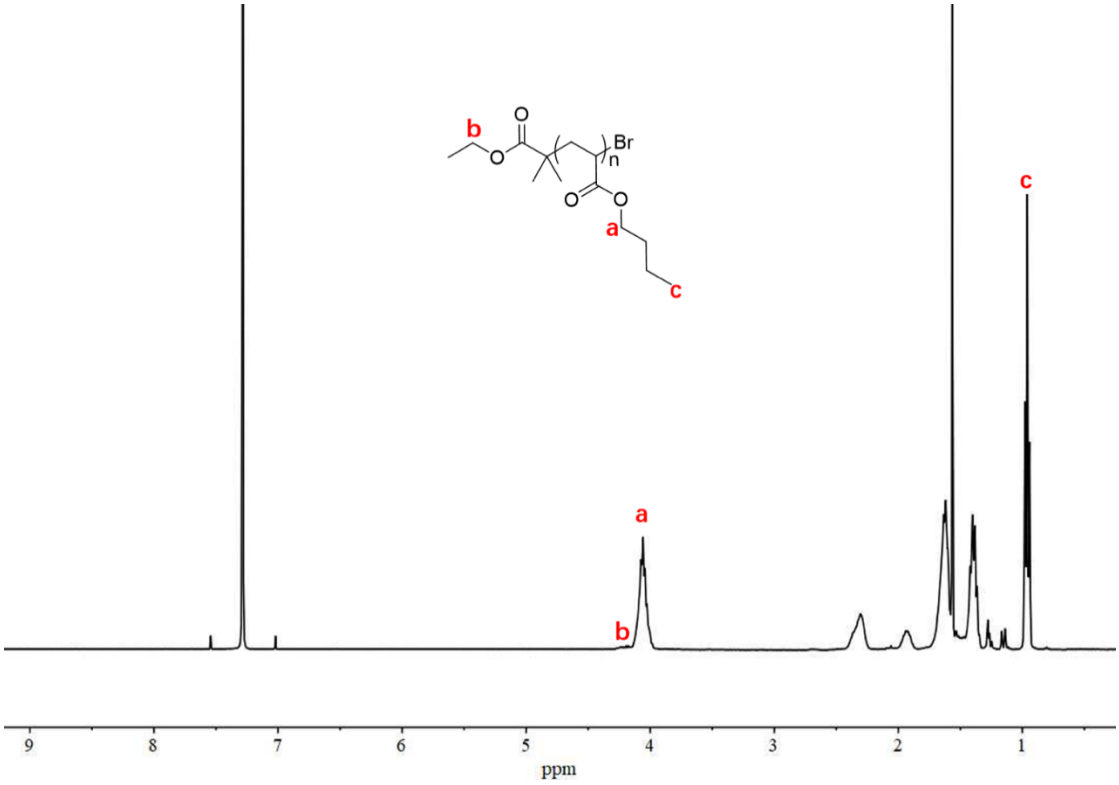

Figure S1. ^{1}H NMR spectrum of **poly(nBuA)$_{40}$-Br** in $CDCl_3$.

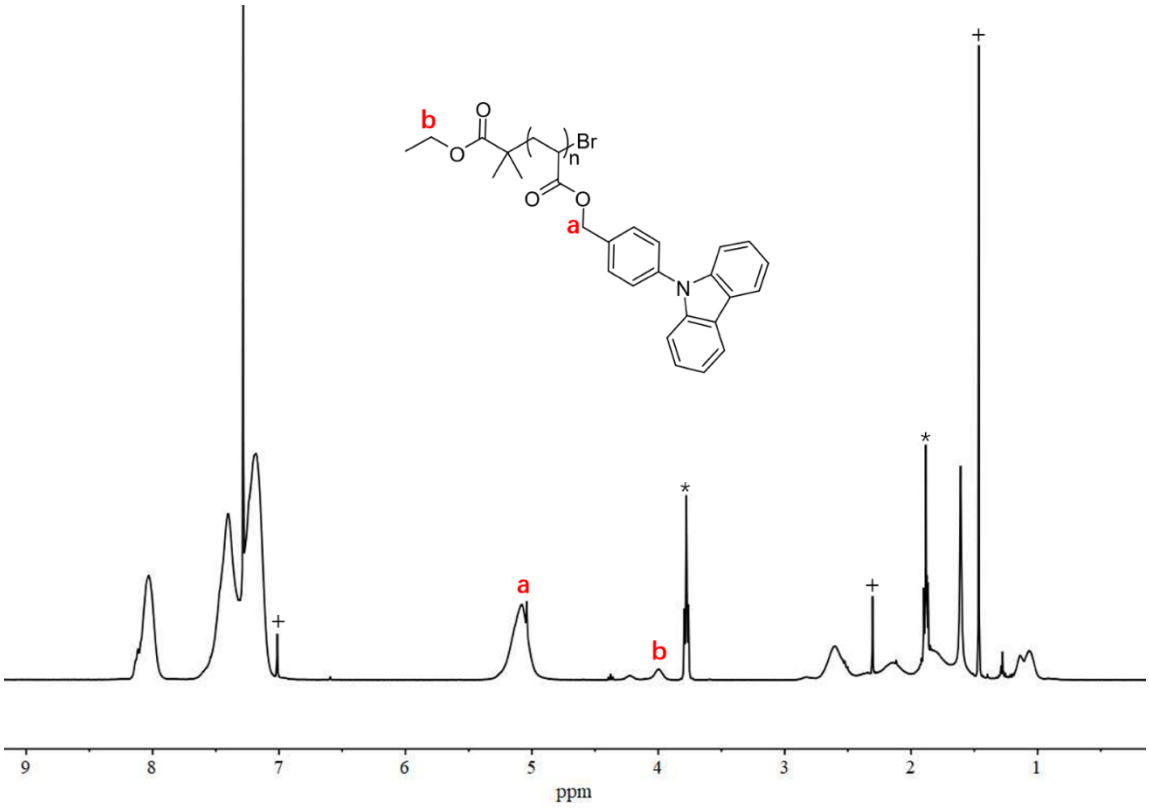

Figure S2. ^{1}H NMR spectrum of **poly(CzBA)$_{15}$-Br** in $CDCl_3$. * = THF; + = BHT.

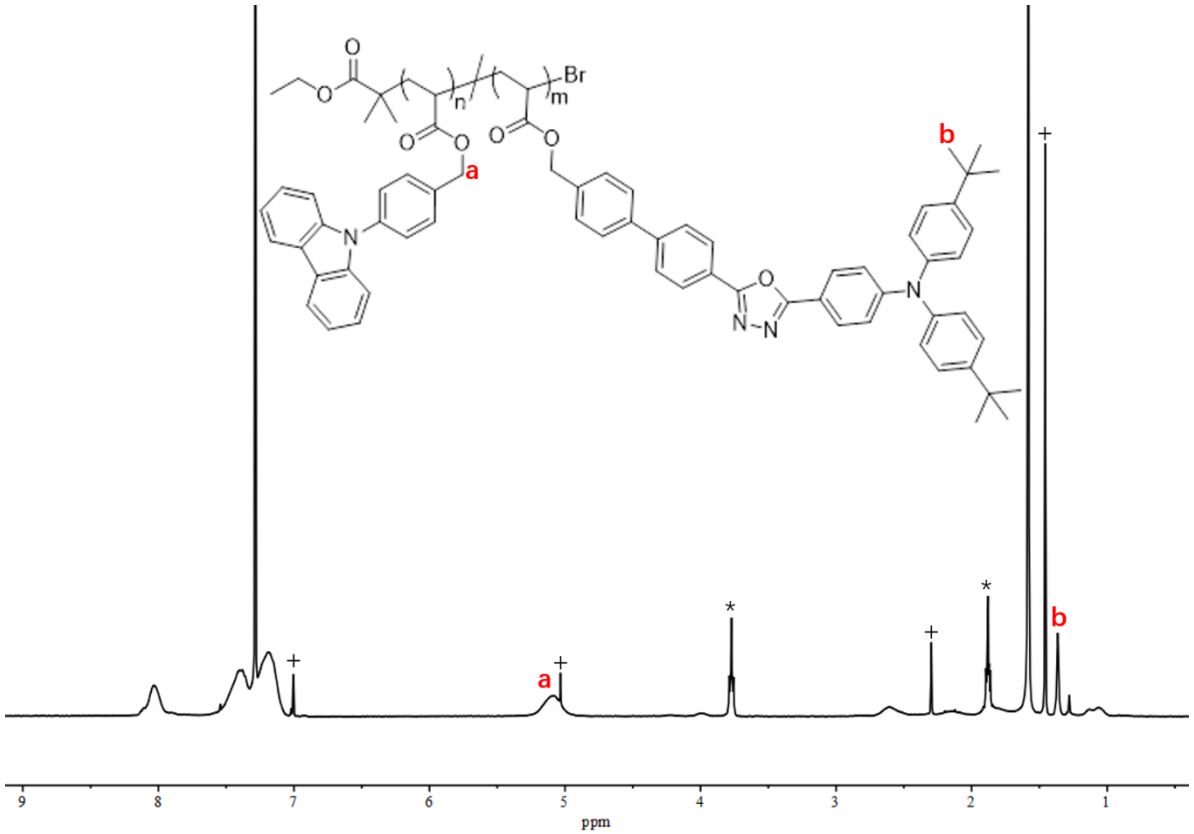

Figure S3. ^{1}H NMR spectrum of **poly(CzBA-*co*-PAPOMA)$_{15}$-Br** in $CDCl_3$. * = THF; + = BHT.

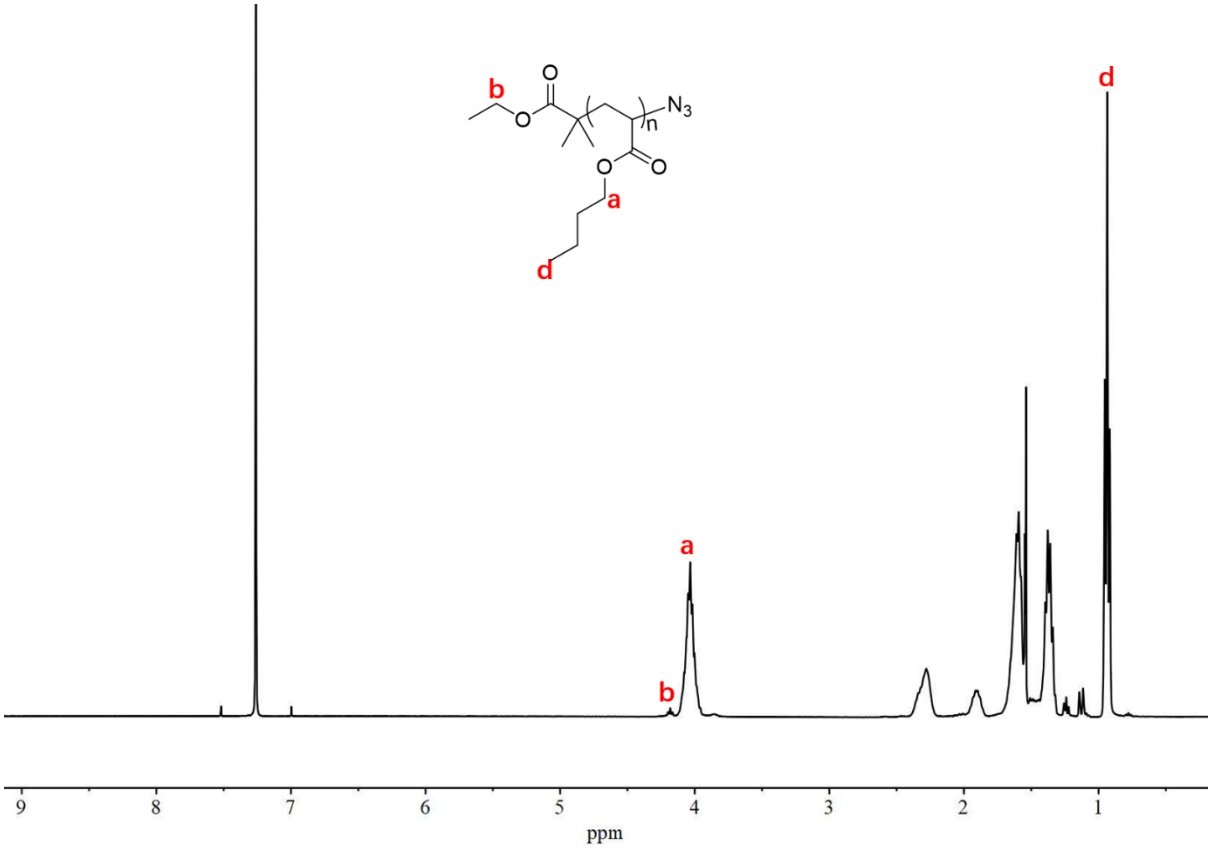

Figure S4. ^{1}H NMR spectrum of **poly(nBuA)$_{40}$-N$_3$** in $CDCl_3$.

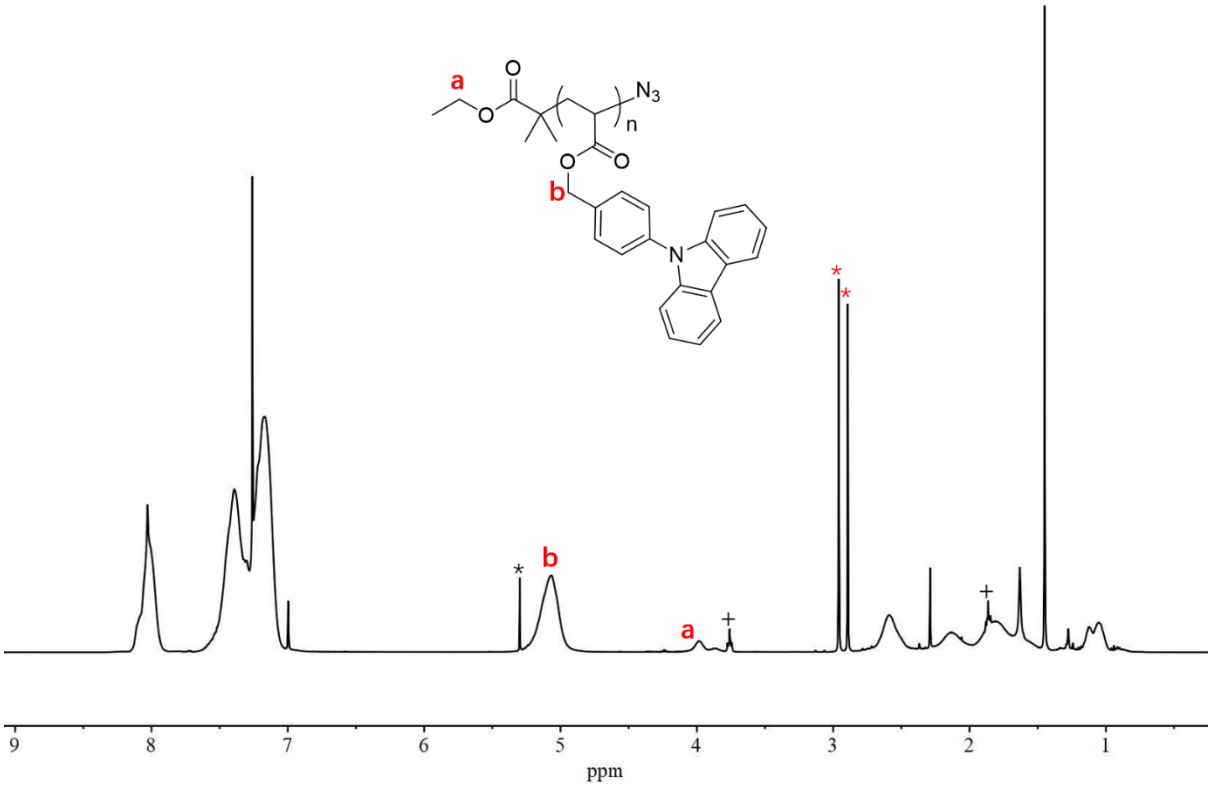

Figure S5. ^{1}H NMR spectrum of **poly(CzBA)$_{15}$-N$_3$** in $CDCl_3$. * = DCM; + = THF; * = DMF.

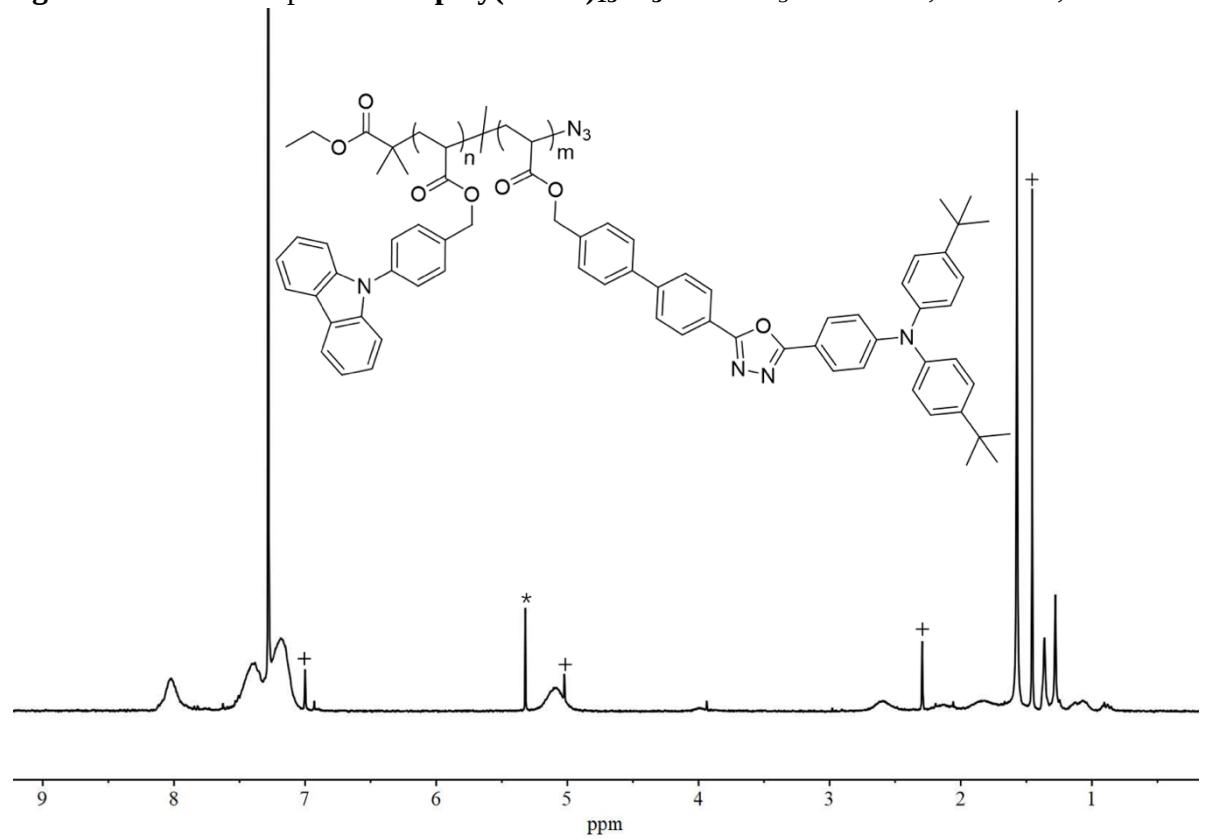

Figure S6. ^{1}H NMR spectrum of **poly(CzBA-co-PAPOMA)$_{15}$-N$_3$** in $CDCl_3$. * = DMF; + = BHT.

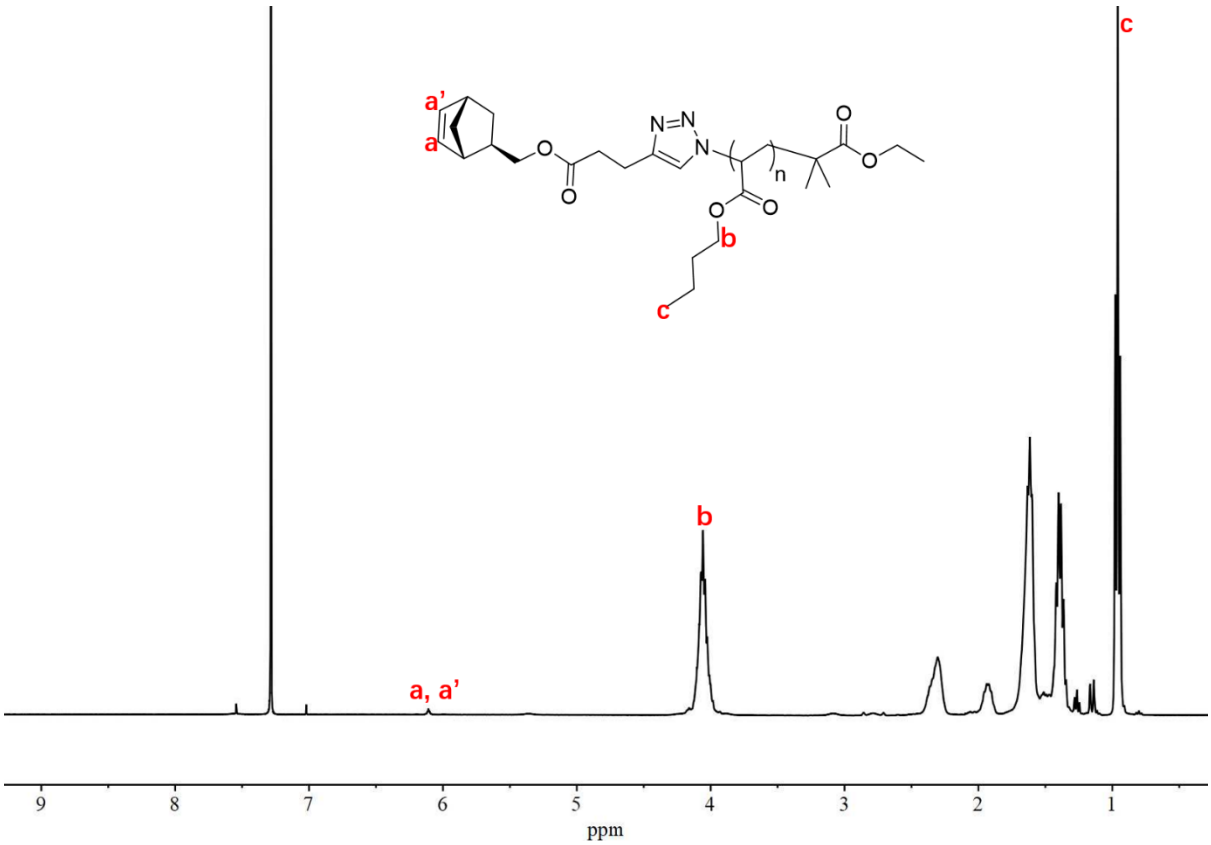

Figure S7. ^{1}H NMR spectrum of **nBuA-MM** in $CDCl_3$.

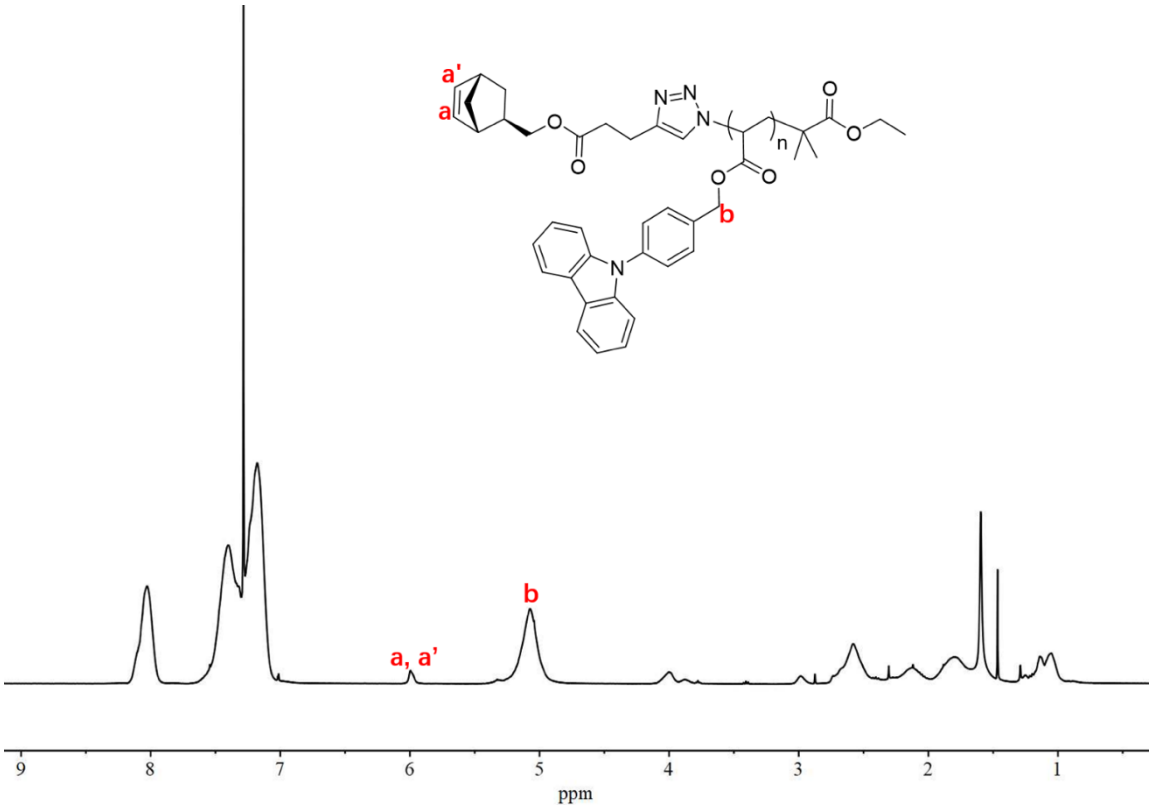

Figure S8. ^{1}H NMR spectrum of **CzBA-MM** in $CDCl_3$.

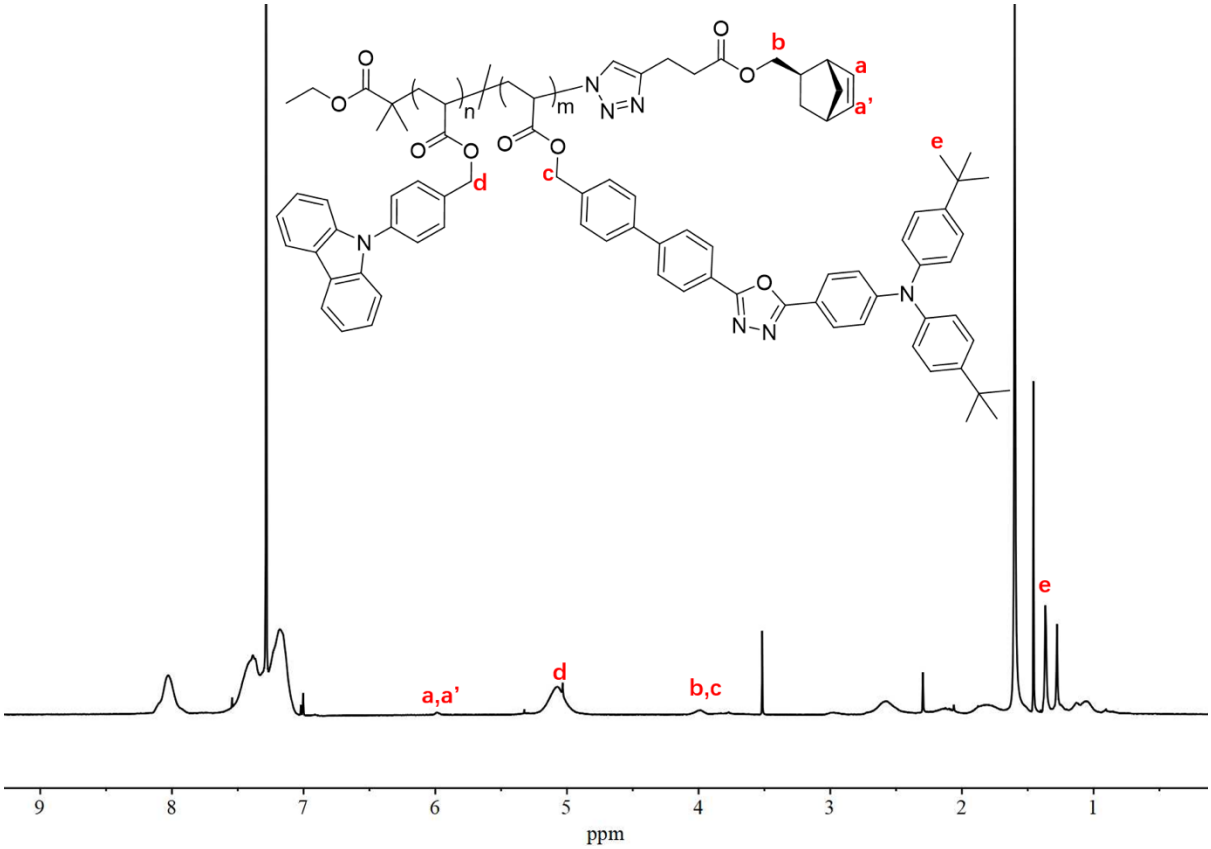

Figure S9. ^{1}H NMR spectrum of **(CzBA-*co*-PAPOMA)-MM** in $CDCl_3$.

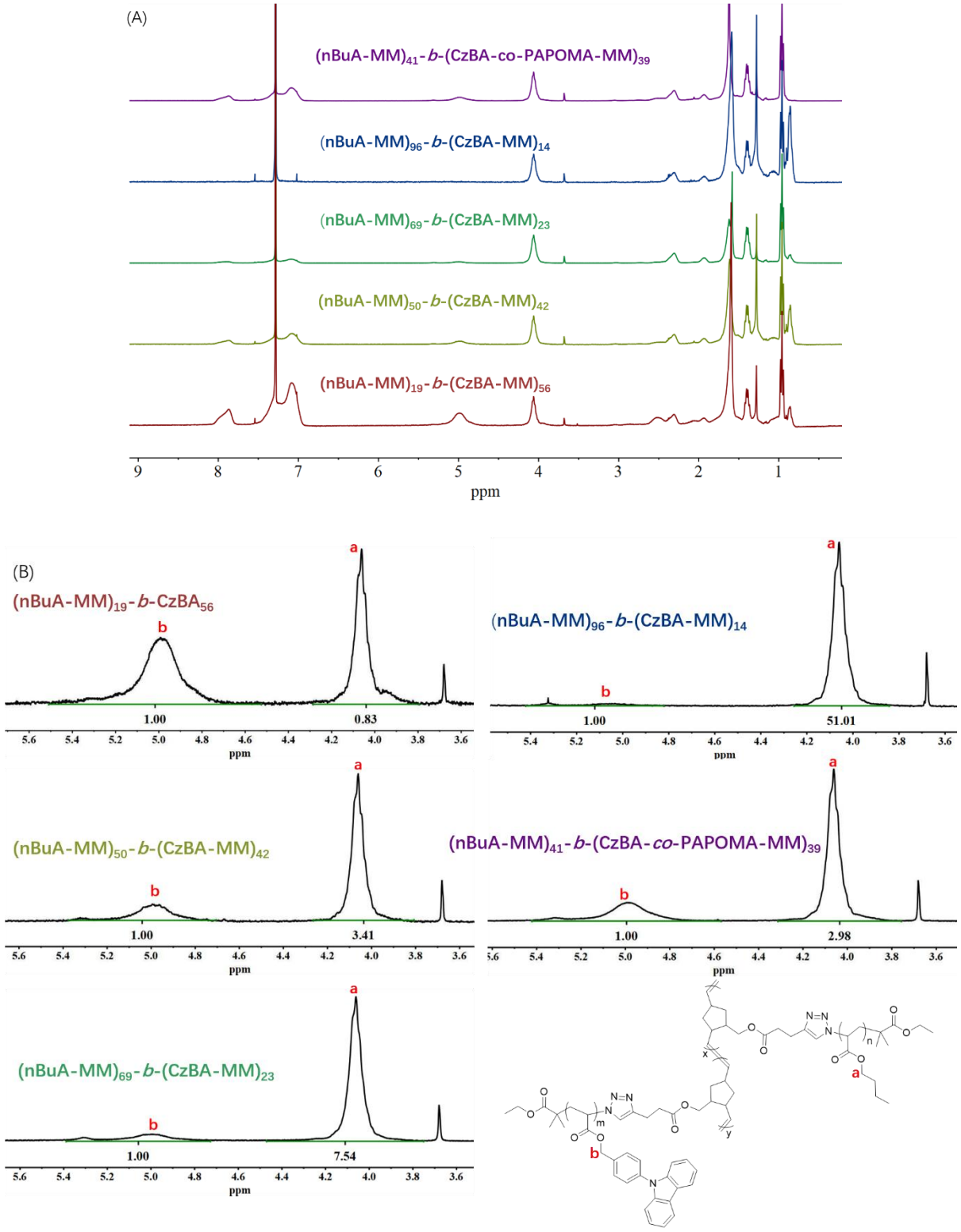

Figure S10. ^{1}H NMR spectrum of bottlebrush diblock copolymers in $CDCl_3$. The integrated areas of peaks a and b were used to determine the degree of polymerization of poly(norbornene) backbone for the **CzBA-MM** block. For the first block **nBuA-MM**, the degree of polymerization of the poly(norbornene) backbone was determined by SEC.

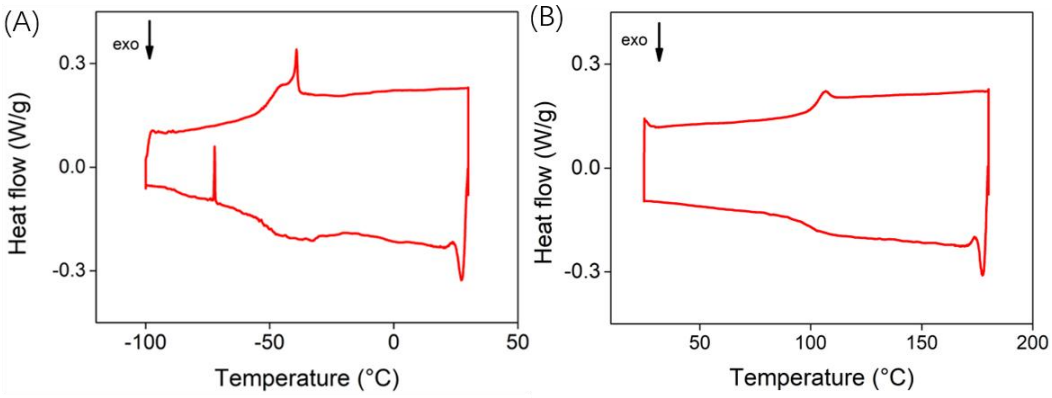

Figure S11. DSC traces of macromonomers (A) **nBuA-MM** and (B) **CzBA-MM** run at a rate of 10 °C min^{-1} under a 60 mL min^{-1} flow of nitrogen. Two consecutive heating and cooling cycles were performed, the second is shown.

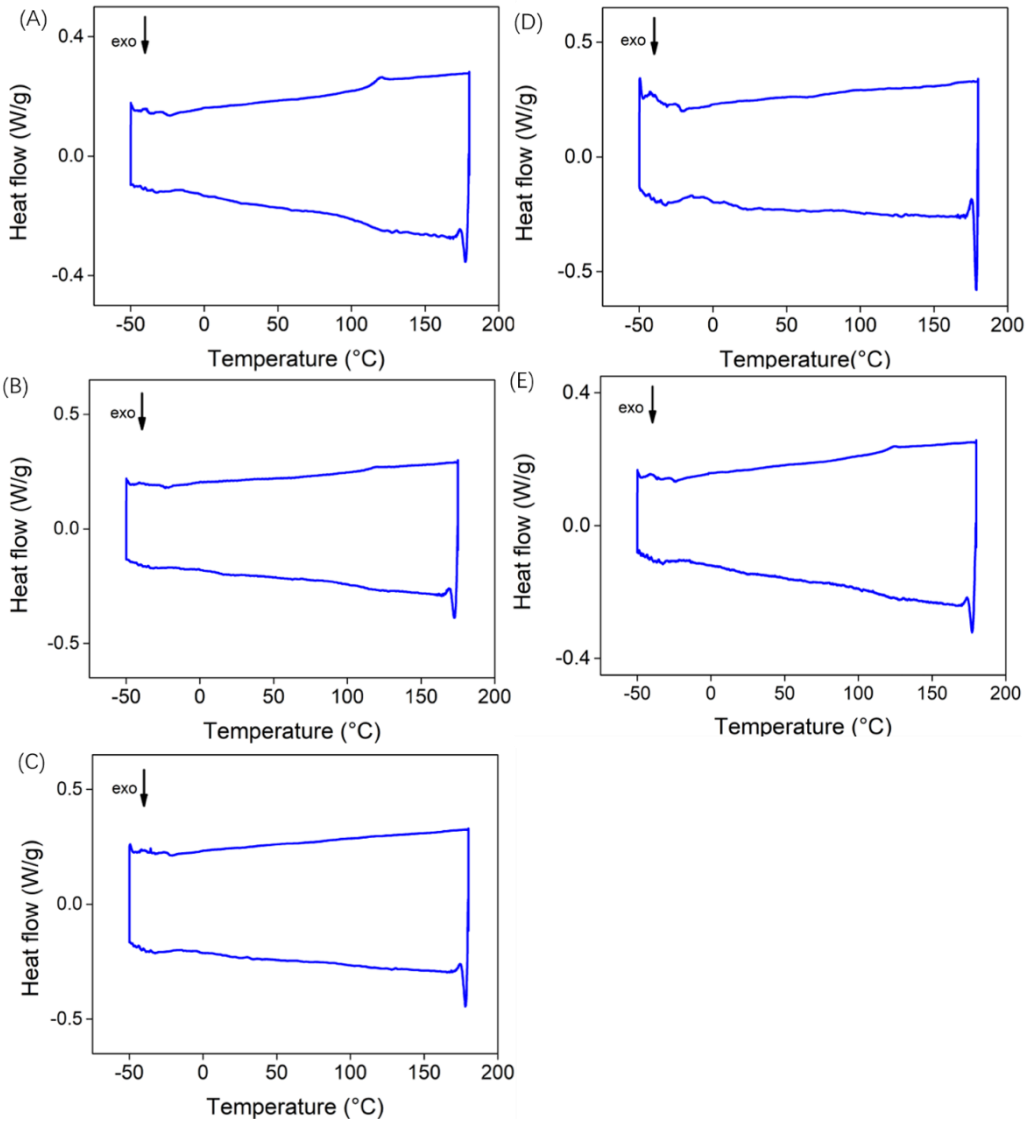

Figure S12. DSC traces of bottlebrush diblock copolymers (A) **(nBuA-MM)$_{19}$-*b*-(CzBA-MM)$_{56}$**, (B) **(nBuA-MM)$_{50}$-*b*-(CzBA-MM)$_{42}$**, (C) **(nBuA-MM)$_{69}$-*b*-(CzBA-MM)$_{23}$**, (D) **(nBuA-MM)$_{96}$-*b*-(CzBA-MM)$_{14}$**, (E) **(nBuA-MM)$_{41}$-*b*-(CzBA-*co*-PAPOMA-MM)$_{39}$**

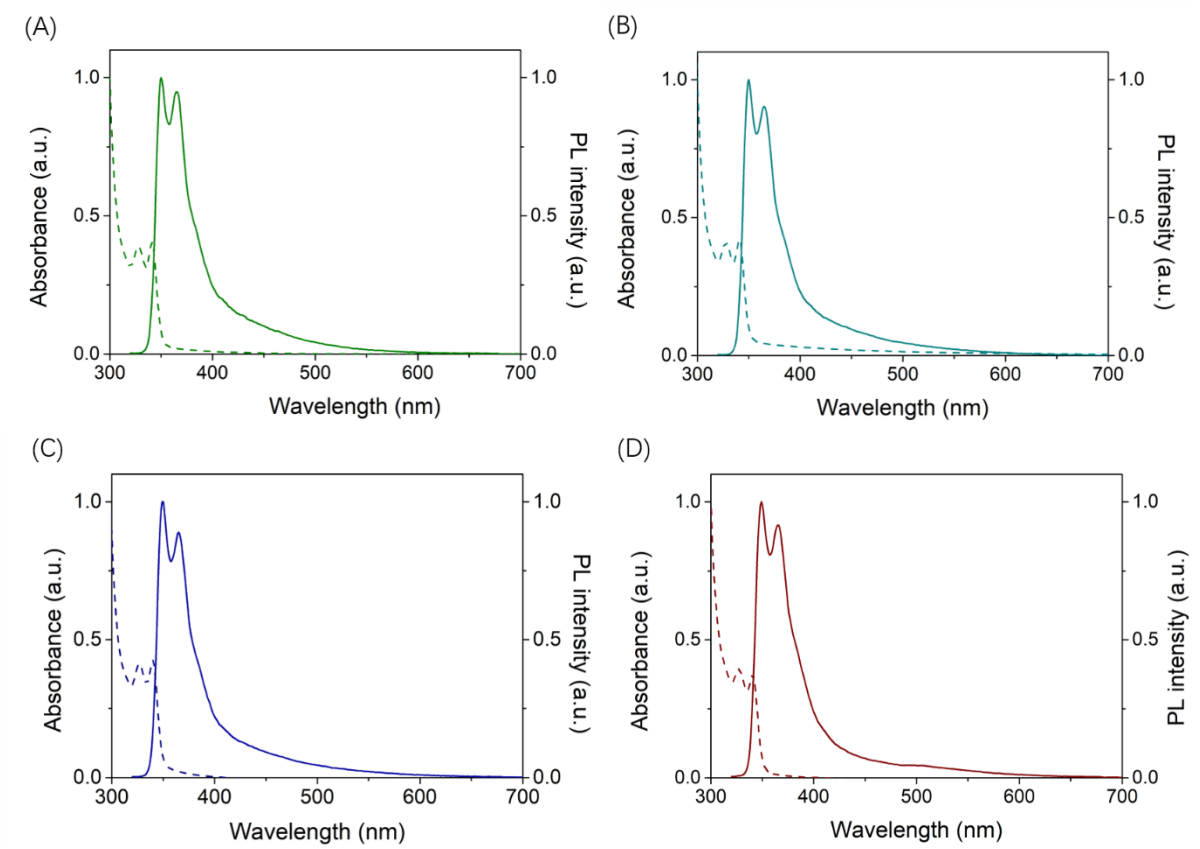

Figure S13. Normalized absorbance (dashed) and photoluminescence (solid) spectra for micelles of bottlebrush diblock copolymers (A) **(nBuA-MM)$_{19}$-*b*-(CzBA-MM)$_{56}$**, (B) **(nBuA-MM)$_{50}$-*b*-(CzBA-MM)$_{42}$**, (C) **(nBuA-MM)$_{69}$-*b*-(CzBA-MM)$_{23}$**, (D) **(nBuA-MM)$_{96}$-*b*-(CzBA-MM)$_{14}$**, in trifluoroethanol at 0.1 mg/mL. λ_{ex} = 300 nm.

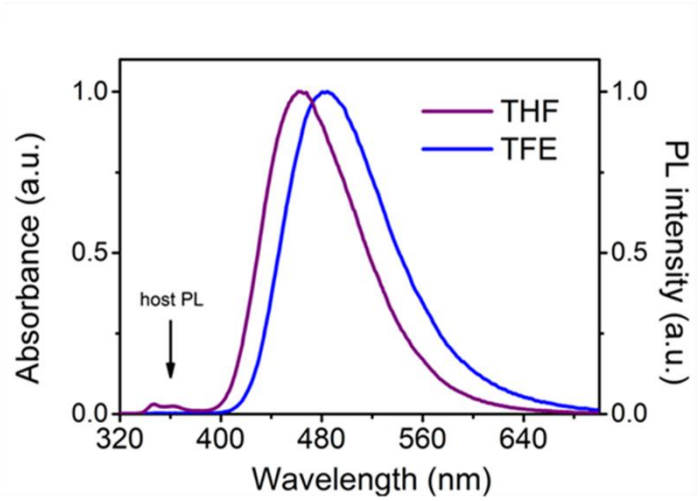

Figure S14. Emission spectra for **(nBuA-MM)$_{41}$-*b*-(CzBA-*co*-PAPOMA-MM)$_{39}$** at 0.1 mg/mL in THF and TFE. λ_{ex} = 300 nm

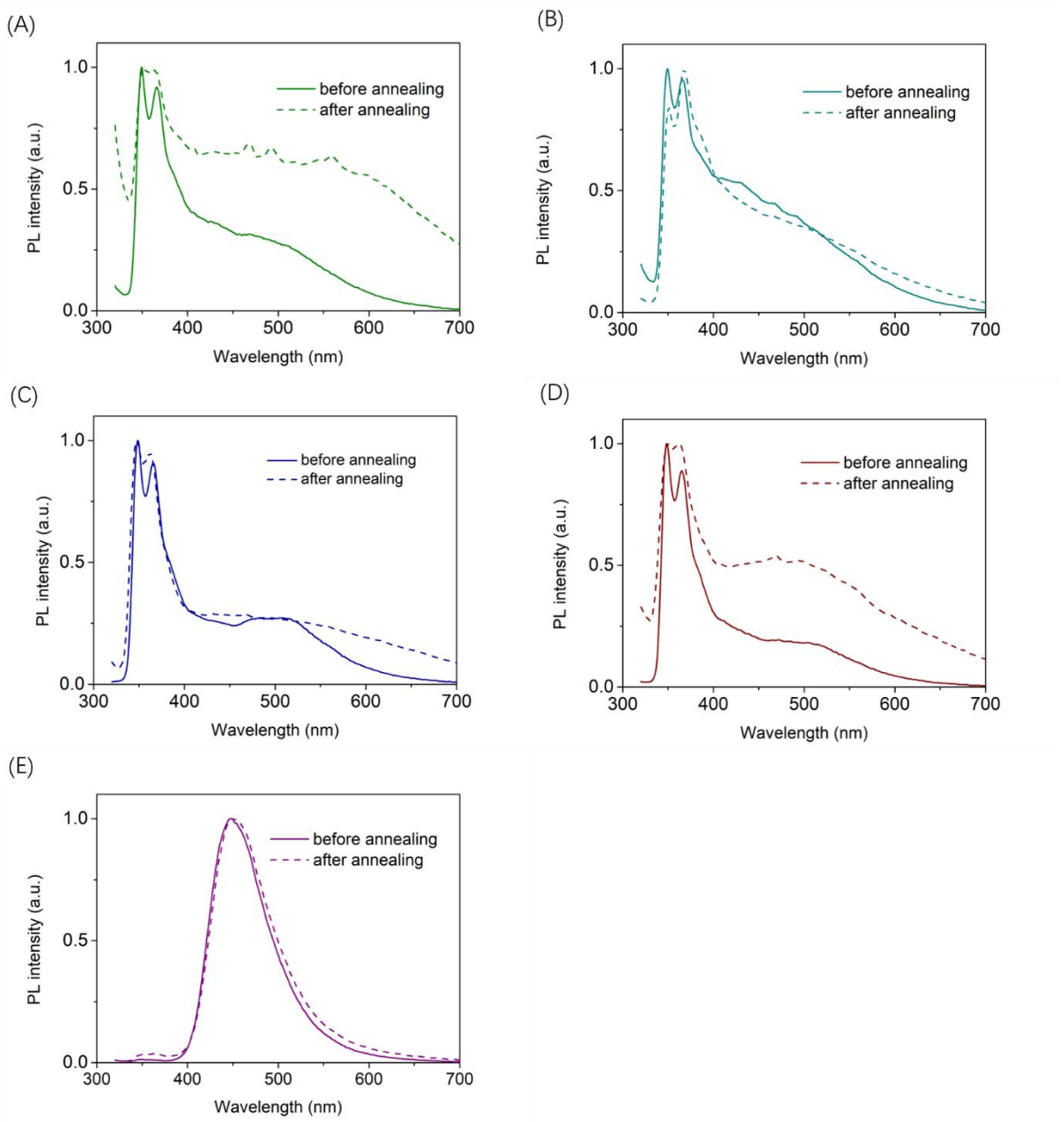

Figure S15. Solid state photoluminescence spectra of bottlebrush diblock copolymers (A) **(nBuA-MM)$_{19}$-*b*-(CzBA-MM)$_{56}$**, (B) **(nBuA-MM)$_{50}$-*b*-(CzBA-MM)$_{42}$**, (C) **(nBuA-MM)$_{69}$-*b*-(CzBA-MM)$_{23}$**, (D) **(nBuA-MM)$_{96}$-*b*-(CzBA-MM)$_{14}$**, (E) **(nBuA-MM)$_{41}$-*b*-(CzBA-*co*-PAPOMA-MM)$_{39}$**, before (solid) and after (dashed) annealing. Spin-coated on quartz glass substrates. Annealed at 150 °C. λ_{ex} = 293 nm.

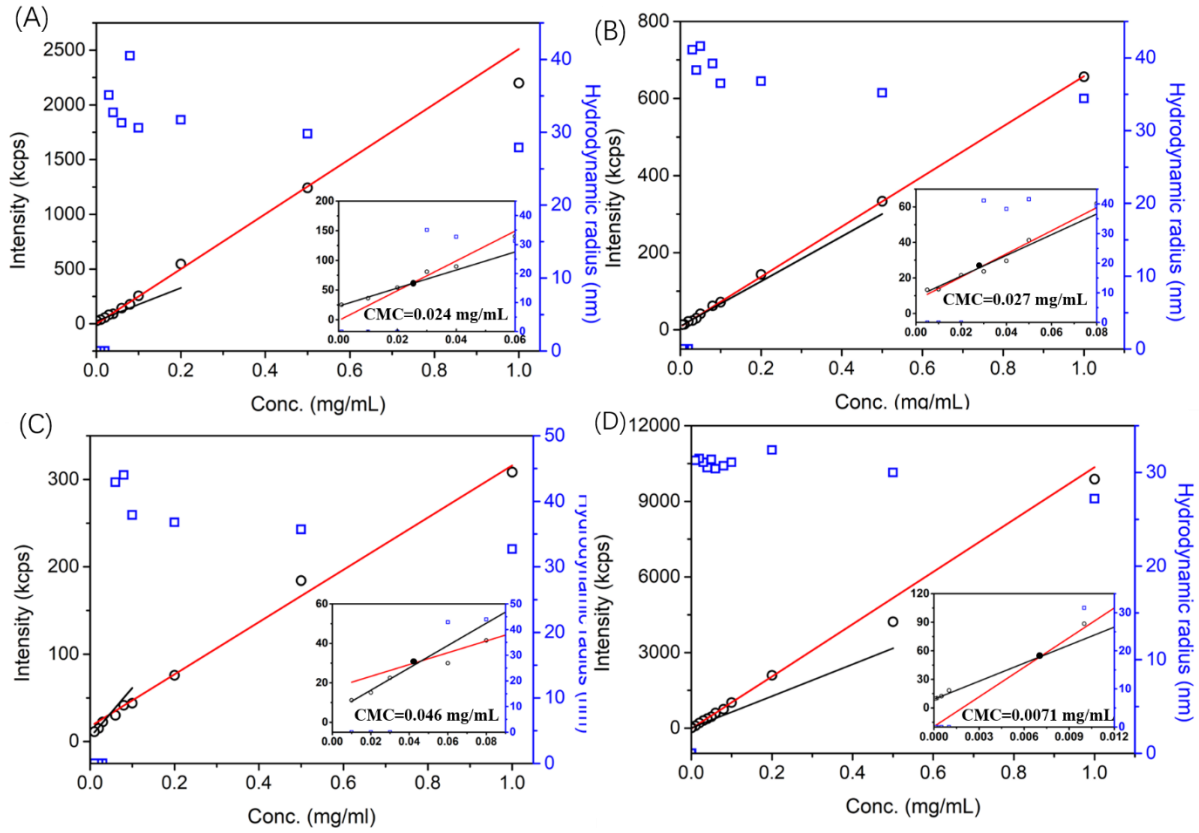

Figure S16. Dynamic light scattering plots of intensity of scattered light (black circle) and hydrodynamic radius (blue square) obtained for bottlebrush diblock copolymers (A) **(nBuA-MM)$_{19}$-*b*-(CzBA-MM)$_{56}$**, (B) **(nBuA-MM)$_{69}$-*b*-(CzBA-MM)$_{23}$**, (C) **(nBuA-MM)$_{96}$-*b*-(CzBA-MM)$_{14}$**, (D) **(nBuA-MM)$_{41}$-*b*-(CzBA-*co*-PAPOMA-MM)$_{39}$**, at various concentrations in trifluoroethanol. The intersection of the two lines in the intensity data corresponds to the critical micelle concentration (CMC).

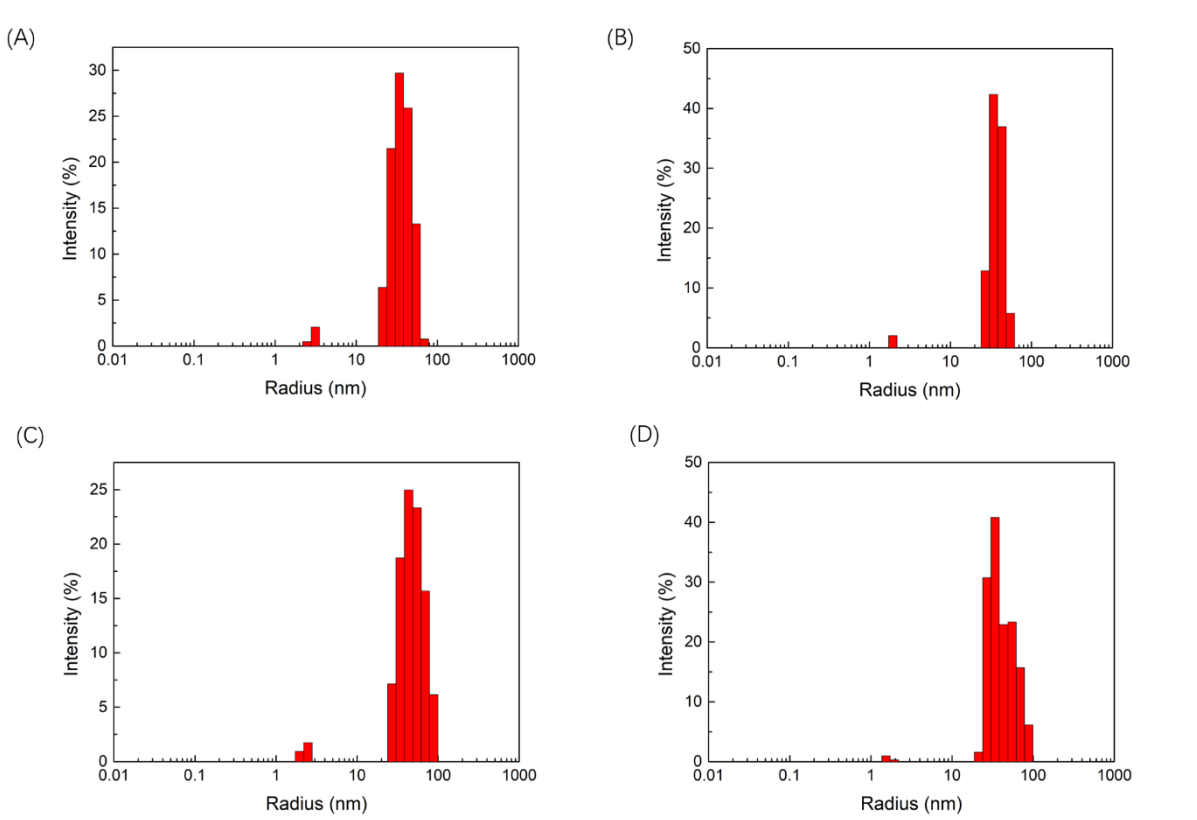

Figure S17. Size distribution by dynamic light scattering for micelles of bottlebrush diblock copolymers (A) (**nBuA-MM)$_{19}$-*b*-(CzBA-MM)$_{56}$**, (B) (**nBuA-MM)$_{69}$-*b*-(CzBA-MM)$_{23}$**, (C) (**nBuA-MM)$_{96}$-*b*-(CzBA-MM)$_{14}$**, (D) (**nBuA-MM)$_{41}$-*b*-(CzBA-*co*-PAPOMA-MM)$_{39}$** at 0.06 mg/mL in TFE.

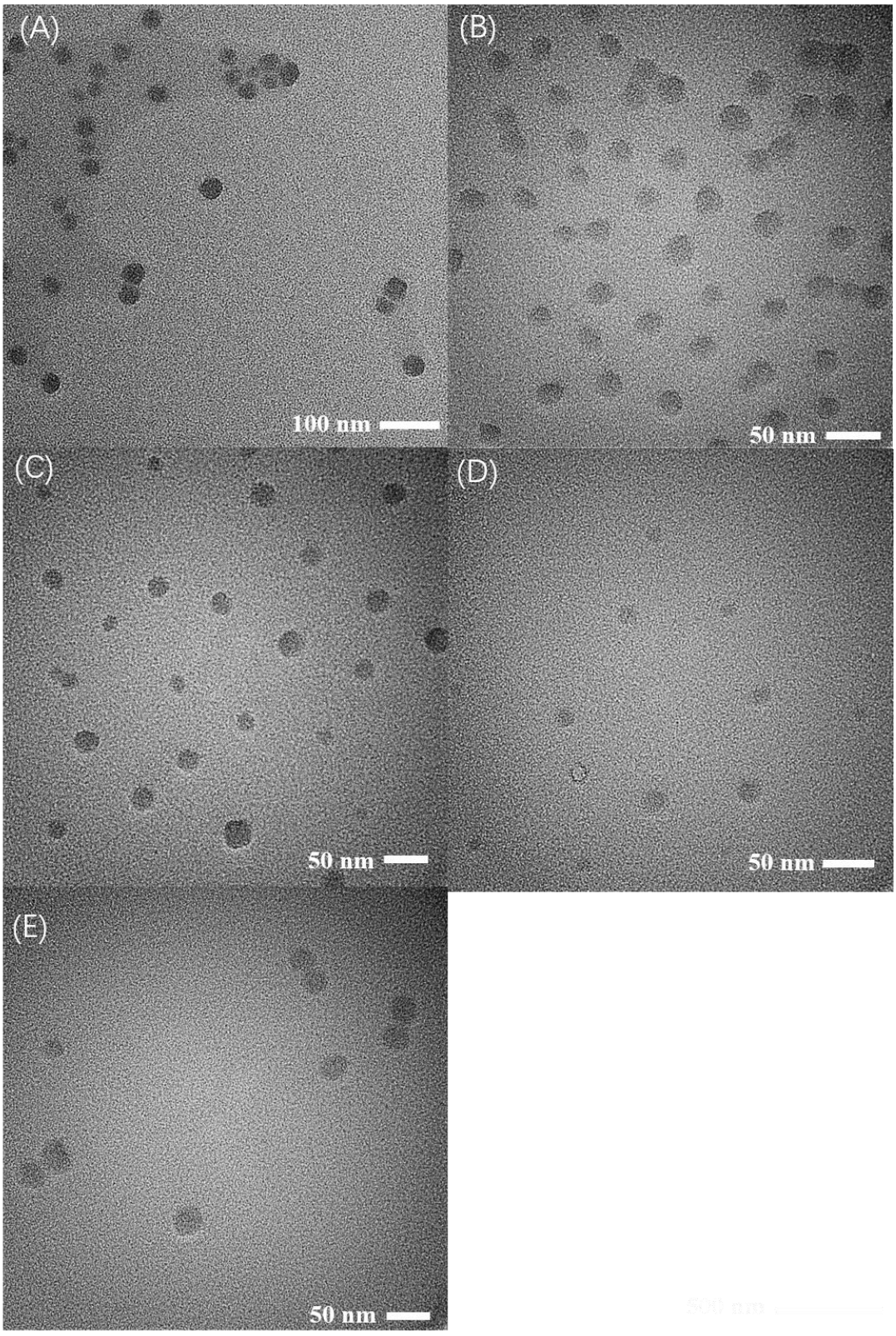

Figure S18. TEM images of micelles (A) **(nBuA-MM)$_{19}$-*b*-(CzBA-MM)$_{56}$**, (B) **(nBuA-MM)$_{50}$-*b*-(CzBA-MM)$_{42}$**, (C) **(nBuA-MM)$_{69}$-*b*-(CzBA-MM)$_{23}$**, (D) **(nBuA-MM)$_{96}$-*b*-(CzBA-MM)$_{14}$**, (E) **(nBuA-MM)$_{41}$-*b*-(CzBA-*co*-PAPOMA-MM)$_{39}$**. Micelles were formed at 0.06 mg/ml in TFE and dried for TEM imaging.

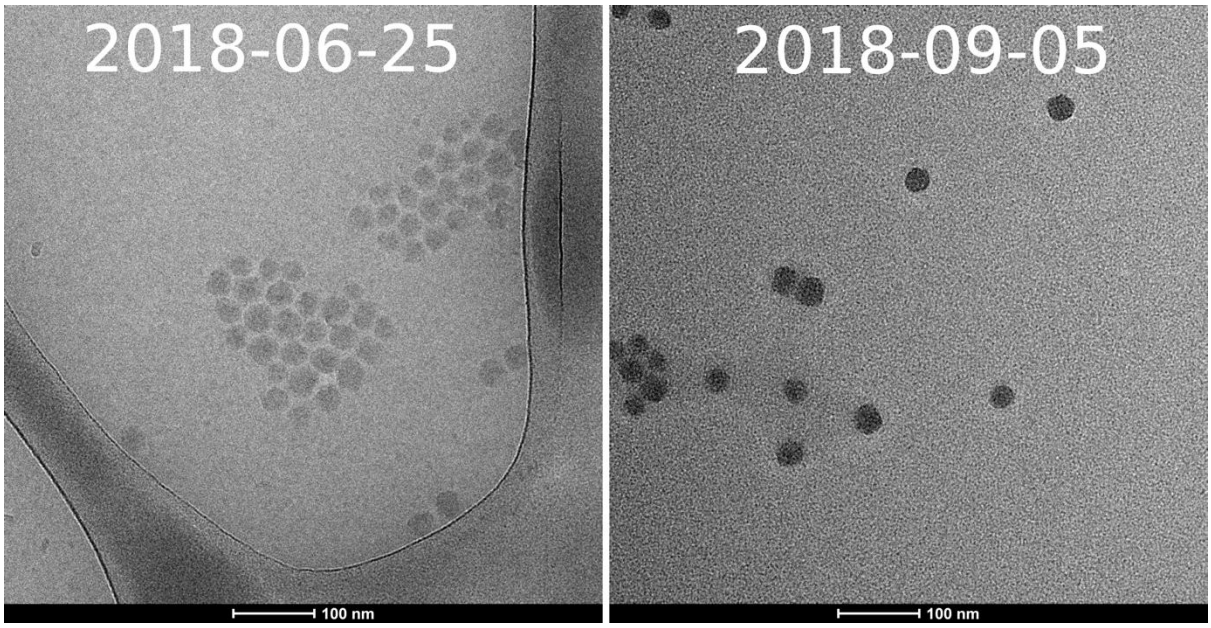

Figure S19. Cryo-TEM (left) and TEM (right) images of micelles for (**nBuA-MM)$_{19}$-*b*-(CzBA-MM)$_{56}$**. Micelles were formed at 0.08 mg/mL in TFE and dried for TEM imaging.

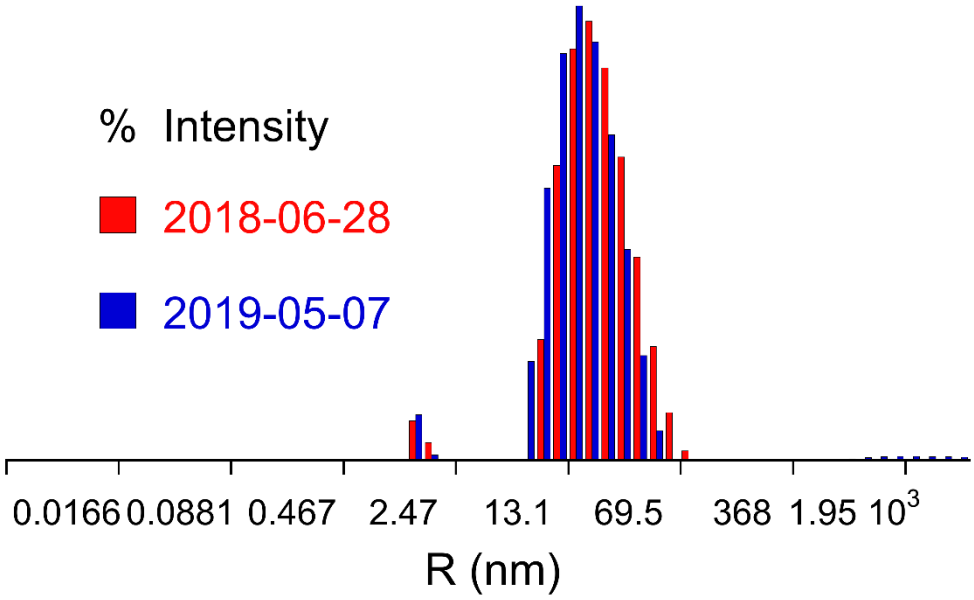

Figure S20. Size distribution by dynamic light scattering for micelles of bottlebrush diblock copolymers (**nBuA-MM)$_{19}$-*b*-(CzBA-MM)$_{56}$** with the 0.08 mg mL^{-1} solution stood for more than ten months.

Additional Tables

Table S1 Synthesis of prepolymers.

Entry	M_n[a] (Da)	DP[a]	[M/I][b]	$Đ$[a]	Conv. (%)[c]
Poly(nBuA)$_{40}$-Br	5200	39	40	1.16	95
Poly(CzBA)$_{15}$-Br	4800	13	15	1.16	78
Poly(CzBA-*co*-PAPOMA)$_{15}$-Br	5700	14	15	1.12	73

[a]Determined by SEC in THF.
[b]Monomer to initiator ratio.
[c]Determined using ^{1}H NMR.

Table S2. Synthesis of macromonomers.

Entry	M_n (Da)	$Đ$
nBuA-MM	5600	1.14
CzBA-MM	5200	1.15
(CzBA-*co*-PAPOMA)-MM	6000	1.12

Table S3. Polymer photophysical properties.

Entry	$\lambda_{max, abs}$[a]	$\lambda_{max, em}$[a]	$\lambda_{max, em}$, before annealing	$\lambda_{max, em}$, after annealing
(nBuA-MM)$_{19}$-*b*-(CzBA-MM)$_{56}$	293	350	349	351
(nBuA-MM)$_{50}$-*b*-(CzBA-MM)$_{42}$	293	350	349	368
(nBuA-MM)$_{69}$-*b*-(CzBA-MM)$_{23}$	293	350	349	348
(nBuA-MM)$_{96}$-*b*-(CzBA-MM)$_{14}$	293	349	348	362
(nBuA-MM)$_{41}$-*b*-((CzBA-*co*-PAPOMA)-MM)$_{39}$	293	484	449	448

Concentrations = 0.1 mg mL^{-1}. [a]Measured in TFE. Φ_F was measured in toluene to reduce excimer formation; values ± 0.05.

Table S4. Glass transition temperatures of bottlebrush diblock copolymers.

Entry	$T_{g,\ nBuA}$	$T_{g,\ CzBA}$
(nBuA-MM)$_{19}$-*b*-(CzBA-MM)$_{56}$	-27.9	112.5
(nBuA-MM)$_{50}$-*b*-(CzBA-MM)$_{42}$	-22.4	109.2
(nBuA-MM)6$_{9}$-*b*-(CzBA-MM)$_{23}$	-25.7	-[a]
(nBuA-MM)$_{96}$-*b*-(CzBA-MM)$_{14}$	-32.6	-[a]
(nBuA-MM)$_{41}$-*b*-((CzBA-*co*-PAPOMA)-MM)$_{39}$	-26.3	119.3

[a]Not observed.